Hybrid GaN LED with capillary-bonded II-VI MQW color-converting membrane for Visible Light Communications

Joao M. M. Santos[1], Brynmor E. Jones[1], Peter J. Schlosser[1], Scott Watson[2], Johannes Herrnsdorf[1], Benoit Guilhabert[1], Jonathan J. D. McKendry[1], Joel De Jesus[3], Thor A. Garcia[4], Maria C. Tamargo[4], Anthony E. Kelly[2], Jennifer E. Hastie[1], Nicolas Laurand[1] and Martin D. Dawson[1]

[1]Institute of Photonics, SUPA, University of Strathclyde, 106 Rottenrow, Glasgow G4 0NW, UK
[2]School of Engineering, University of Glasgow, Glasgow, G12 8LT, UK
[3]Department of Physics, The Graduate Center and The City College of New York, CUNY, New York, NY 10031, USA
[4]Department of Chemistry, City College of New York, 138th Street and Convent Avenue, New York, NY 10031, USA

E-mail : joao.santos@strath.ac.uk

Abstract

The rapid emergence of gallium-nitride (GaN) light-emitting diodes for solid-state lighting has created a timely opportunity for optical communications using visible light. One important challenge to address this opportunity is to extend the wavelength coverage of GaN LEDs without compromising their modulation properties. Here, a hybrid source for emission at 540 nm consisting of a 450nm GaN micro-sized LED (micro-LED) with a micron-thick ZnCdSe/ZnCdMgSe multi-quantum-well color-converting membrane is reported. The membrane is liquid-capillary-bonded directly onto the sapphire window of the micro-LED for full hybridization. At an injection current of 100 mA, the color-converted power was found to be 37 μW. At this same current, the -3dB optical modulation bandwidth of the bare GaN and hybrid micro-LEDs were 79 MHz and 51 MHz, respectively. The intrinsic bandwidth of the color-converting membrane was found to be power-density independent over the range of the micro-LED operation at 145 MHz, which corresponds to a mean carrier lifetime of 1.9 ns.

1. Introduction

Development of light-emitting diode (LED) technology is driven mainly by the need for efficient solid-state lighting, but it is also creating opportunities for new applications such as visible light communications (VLC) [1]. VLC requires light sources that are not only efficient but also have high modulation bandwidth and are wavelength versatile. White-emitting LEDs, and color-converted LEDs in general, are typically obtained by combining blue InGaN LEDs with down-converting phosphors. This approach is effective for illumination purposes but is not well suited to VLC because of the long (μs) excited-state lifetime of phosphors. The resulting sources have modulation bandwidths limited to ~ 1 MHz, whereas unconverted blue InGaN-based LEDs have bandwidths of 20 MHz up to 400 MHz depending on their formats, with single-color direct-LED-emission data links at > 1Gbit/s rate having been demonstrated [2]. There is therefore a need to explore color-converting materials with shorter excited-state lifetimes to complement rare-earth phosphors. Organic semiconductors and colloidal quantum dots are potential candidates but they necessitate advanced encapsulation schemes for long-term environmental stability [3].

Here we introduce an alternative approach based on using inorganic MQW semiconductor epi-layer membranes as photo-pumped color converters for the underlying InGaN LEDs. This technology benefits from being based on all-inorganic semiconductors and therefore promises to be robust [4], [5]. It also leads to extremely compact sources, as the membrane can be integrated (as we show) by techniques such as liquid capillary bonding. There are several options for wavelength coverage across the visible spectrum with available semiconductor alloys for MQW membranes including III-V AlGaInP (yellow to

red) and InGaN (green) materials and II-VI CdMgZnSe (green to orange) materials [4], [6]. As proof-of-principle of a generic approach, the hybrid LED demonstrator discussed here is obtained by capillary-bonding a 540nm-emitting, II-VI CdMgZnSe MQW membrane onto an array of 450nm InGaN micro-size LEDs (micro-LEDs), on the sapphire side, taking advantage of the high modulation bandwidths associated with these small-sized LEDs [7]. Micro-LEDs operate in a size regime where physical characteristics that play a major role for VLC, e.g. current density, differential carrier lifetime and junction capacitance, diverge from those of conventional format broad area LEDs. This size regime firmly applies to devices with dimensions of 100 µm (as used in this work) and below, where devices can handle kA/cm^2 of DC current density and possess significantly higher modulation bandwidths [7]. We chose II-VI materials for converters in this initial study because (i) they are readily wet etched into epitaxial membranes, (ii) they can be designed to offer coverage of the visible spectrum promising white-light generation, and (iii) they permit an alternative approach to green emission at high-modulation-bandwidth, useful for e.g. introducing coarse wavelength division multiplexing (blue and green) into optical wireless and polymer optical fiber communications.

In the following, the hybrid device fabrication and characterization methods are described in section 2. Sections 3 and 4 report and discuss, respectively, the continuous-wave (CW) and dynamic characteristics of the hybrid source.

2. Device fabrication and characterization

2.1 Device design and fabrication

The 450nm-wavelength micro-LEDs used to pump the MQW membrane were fabricated using a commercial p-i-n GaN LED structure grown on c-plane sapphire, following the procedure reported in [8]. Here, the fabricated chip is made of several 100 µm x 100 µm square micro-LEDs spaced 450 µm apart, Figure 1. After fabrication, the chip was placed onto a printed circuit board and wire bonded to tracks connected to SMA connectors, such that the micro-LEDs could be addressed individually.

The II-VI MQW membrane structure was grown by molecular beam epitaxy on an InP substrate and InGaAs growth buffer. It consists of 9 ZnCdSe quantum wells with CdMgZnSe barriers and was designed to absorb the pump emission in-barriers. The quantum wells emit at 540 nm in a resonant periodic gain configuration for potential alternative use as a laser gain medium [9]. The InP substrate was removed by a combination of mechanical polishing and wet etch process using a solution of HCl:H_3PO_4 in a ratio of 3:1, followed by the removal of the InGaAs layer with a solution of H_3PO_4:H_2O_2:H_2O, in a ratio of 1:1:6 for maximum etch selectivity with the II-VI material [10]. The epi-side is fixed onto a temporary glass substrate for this step, using a wax, for mechanical support during processing. After substrate removal, the II-VI layer was transferred from the glass and capillary-bonded using deionized water onto the sapphire window of the LEDs to complete the hybrid device [11]. The resulting MQW membranes have a thickness of less than 2.5 µm, and a typical surface area of a few mm^2. Images of the hybrid device and structural membrane layout are shown in Figure 1.

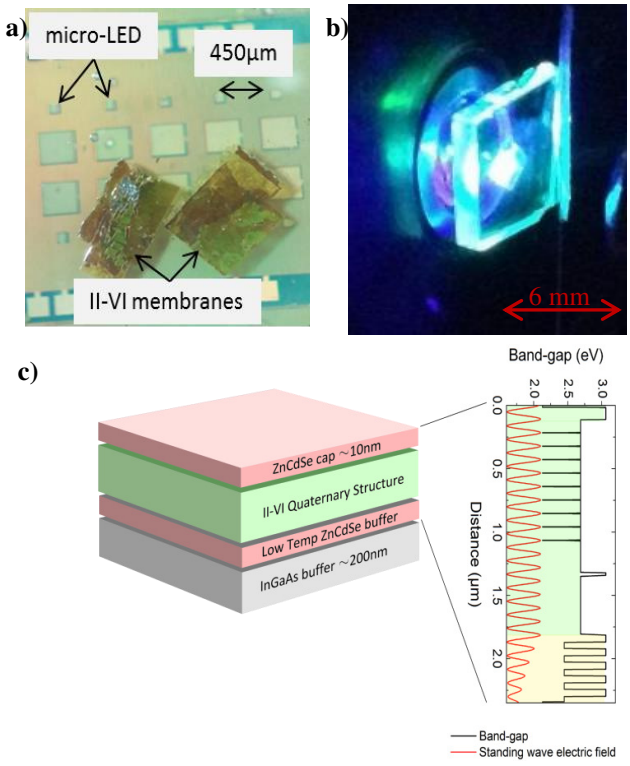

Figure 1 a) Plan view micrograph of the hybrid device. The micro-LED pixels are the smaller elements as labeled, some of which are bonded underneath the II-VI membrane. Between the membrane and the underlying LEDs is the sapphire substrate, b) II-VI membrane when pumped by a blue LED, c) II-VI MQW structural design.

2.2 Experimental Setups

The device was characterized in terms of optical power, emission spectrum and modulation bandwidth prior to and after membrane integration. For the power measurements, the device under test was fixed on top of an optical power meter with a 30mm cage plate in between to enable the optional placement of an optical long-pass filter (500nm cut-off wavelength). Hereafter, in section 3 and 4, we refer to the micro-LED with no membrane as the 'bare LED', the LED with integrated membrane as the 'hybrid micro-LED', and the micro-LED with membrane and filter in place at detection simply as the 'integrated MQW membrane'. Optical spectra were recorded with an Ocean Optics USB4000 Fiber Optic Spectrometer (2.5nm resolution).

For the frequency response and modulation bandwidth measurements, a set of aspheric lenses with focal length of 32 mm and high numerical aperture (NA = 0.612) were used to collect and focus the micro-LED emission into a Femto HSA-X-S-1G4-SI fast photoreceiver (bandwidth of 1.4 GHz). The LED device was simultaneously driven with a dc bias current and a frequency-swept modulated signal (0.250 Vpp) that were combined with a wideband (0.1 to 6000 MHz) Bias-Tee. An Agilent HP 8753ES Network Analyzer was used to provide the modulation signal and to record the device frequency response as detected by the photoreceiver. The long-pass filter was placed before the detection for measurements of the integrated MQW membrane characteristics.

The intrinsic modulation bandwidth of the stand-alone membrane was also characterized as a function of the excitation power density (section 4). For this, the membrane was supported on a glass substrate and remotely pumped with a bare micro-LED. A pair of lenses was placed directly after the bare device to focus its light onto the stand-alone membrane. Further optics were used to collect the light emitted by the membrane and focus it onto the photodetector. A Coherent® BeamMaster was used to measure the micro-LED beam size incident onto the membrane surface and hence to deduce the incident power density. The full width at half maximum (FWHM) spot-size was found to be 330µm. The bandwidth measurement of the stand-alone membrane was otherwise as described above.

3. CW characteristics

Normalized spectral measurements for the bare micro-LED, the hybrid micro-LED and the integrate MQW membrane (i.e. the contribution of the converted light at 540 nm) are presented in Figure 2. The bare micro-LED has emission centered at 445 nm. The hybrid LED spectrum shows a peak centered at 475 nm and a secondary peak at 540 nm. The emission at 540 nm comes from the light emitted by the II-VI MQW membrane. The II-VI membrane is designed to absorb 97 % to 98 % of 450nm monochromatic light. Because of the bandwidth of the bare micro-LED spectrum (23 nm FWHM) the effective micro-LED light absorption is 85% ± 1%. The band-edge of the membrane is at around 460 nm and therefore the long-wavelength tail of the micro-LED emission is not fully absorbed, explaining the 'apparent' 475nm peak in the spectrum of the integrated MQW membrane.

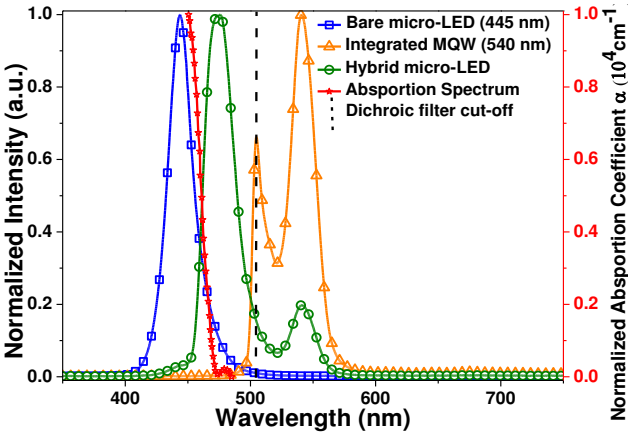

Figure 2. Emission spectra from bare and hybrid pixels and the II-VI band-edge normalized absorption.

The power transfer functions (optical power versus bias current) for the bare, hybrid micro-LEDs and integrated MQW membrane are shown in Figure 3. At 100mA dc, which was found to be the maximum current before thermal rollover, the measured optical powers from the bare micro-LED and the integrate MQW membrane (i.e. the color-converted light contribution) are 4 mW and 37 µW, respectively. The total power of the hybrid micro-LED is 0.58 mW. The power conversion efficiency - defined as the ratio between 540nm over incident 450nm power – was found to be 1% ± 0.1% as derived from the power transfer functions.

The membrane structure used for this initial proof of principle was not primarily designed for color-conversion and the high index contrast between the membrane material and air (2.5:1) results in a significant amount of waveguided light, which is then lost through reabsorption and edge emission. Improved epilayer design of the membrane and implementation of light extraction schemes would improve this value significantly.

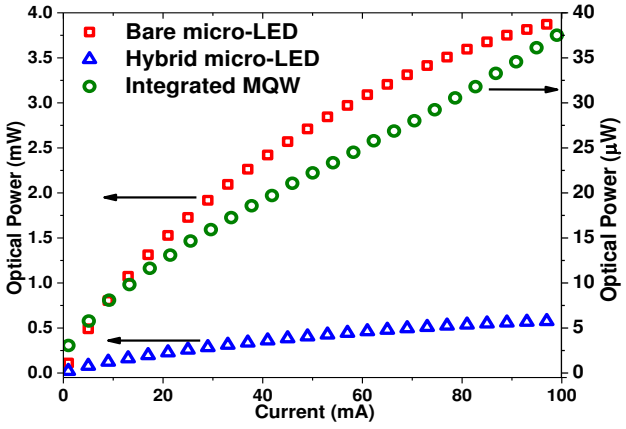

Figure 3. CW optical powers of the bare, hybrid unfiltered micro-LED and integrated MQW membrane.

4. Dynamic characteristics

The modulation properties of the hybrid micro-LED are important for VLC applications and represent the main focus of this study. This section looks into the dynamic characteristics of the bare micro-LED and the MQW membrane and what this implies for the hybrid LED modulation properties.

4.1 Bandwidth measurements

The electrical frequency responses of the bare micro-LED and integrated MQW membrane were measured at different levels of bias current. The -3dB optical bandwidth values (the frequency at which the optical power is half the dc value, f_{co}) was obtained for each bias current by fitting the data, considering a possible multi-exponential decay of the luminescence. The following expressions were used for the fits [12]:

$$N(\omega) = \frac{\sum_i \frac{a_i \omega \tau_i^2}{(1+\omega^2\tau_i^2)}}{\sum_i a_i \tau_i} \quad (1)$$

$$D(\omega) = \frac{\sum_i \frac{a_i \tau_i}{(1+\omega^2\tau_i^2)}}{\sum_i a_i \tau_i} \quad (2)$$

$$M(\omega) = (N(\omega)^2 + D(\omega)^2)^{1/2} \quad (3)$$

In the expressions (1) to (3), the ω and τ_i parameters represent the angular frequency of the modulation and the time constant of the i^{th} exponential decay process, respectively. a_i is a multiplicative factor indicating the contribution strength of the i^{th} decay process. N, D and M are the sine and cosine intensity decay transforms and the demodulation factors [12].

The frequency responses of the bare micro-LED and integrated MQW membrane when driven at 80mA bias current and their corresponding fitting curves are depicted in Figure 4. They are fitted considering a bi-exponential decay of the luminescence, one component of the decay being dominant. The resulting parameters for this particular case are, $a_1 = 0.0037$, $a_2 = 0.9963$, $\tau_1 = 0.2$ µs, $\tau_2 = 3$ ns, $f_{co} = 69$ MHz and $a_1 = 0.0024$, $a_2 = 0.9976$, $\tau_1 = 0.2$ µs, $\tau_2 = 4.6$ ns and $f_{co} = 47$ MHz respectively.

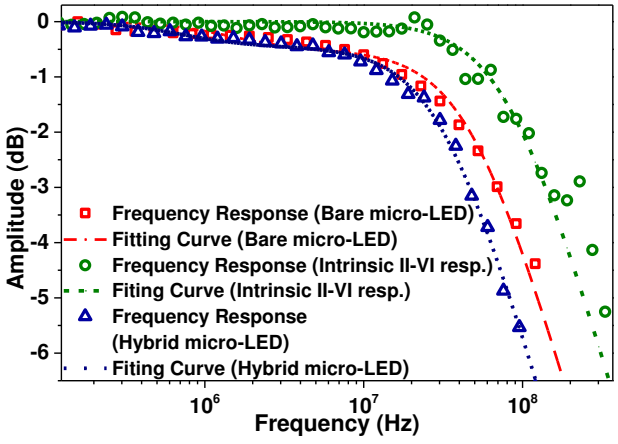

Figure 4. Frequency responses for 80 mA bias current of the bare and hybrid micro-LED, as well as the intrinsic response of the color-converting membrane (integrated MQW membrane), with the respective bi-exponential fits.

The data for the intrinsic response of the color-converting membrane is obtained by removing the frequency response contribution of the bare micro-LED from the overall response of the hybrid device [3]. This is also plotted in Figure 4 along with its fit. This

response is accounted for by a mono-exponential decay of the MQW membrane photoluminescence and its bandwidth is determined by the following bandwidth-lifetime relation,

$$f_{co} = \frac{\sqrt{3}}{2\pi\tau_i} \quad (4)$$

In eq.4, f_{co} is the optical bandwidth and τ_i the photoluminescence lifetime, also the carrier lifetime. The mono-exponential decay parameters found for this curve are, $a_1 = 1$, $\tau_1 = 2.0$ ns and $f_{co} = 139$ MHz.

Figure 5 plots the optical bandwidth values versus the InGaN LED bias current for the bare and hybrid micro-LED as well as the intrinsic modulation bandwidth of the membrane. The data is also summarized in Table 1 along with the respective goodness of fit (GoF) values. The GoF is a statistical analysis that characterizes how well the fit describes the measured data, i.e., is a parameter often used to describe the discrepancy between a set of raw data and a model. With GoF = 1 being a perfect fit and GoF < 1 indicating some discrepancy between data.

Table 1. Table with bandwidth values, f_{co}, for the II-VI membrane (integrated MQW membrane - a long pass filter was used to remove the blue light), the bare micro-LED and the hybrid device, the goodness of fit, GoF and the lifetime, τ_i. *Frequency response obtained through the bare and hybrid LED measurements.

	Bare micro-LED		Intrinsic II-VI membrane response*			Hybrid micro-LED	
I (mA)	f_{co} (MHz)	GoF	f_{co} (MHz)	τ_i (ns)	GoF	f_{co} (MHz)	GoF
5	23±2	0.991	78±15	3.5±1.4	0.947	16±1	0.997
10	29±2	0.988	126±2	2.2±0.1	0.958	23±2	0.995
20	37±2	0.987	191±31	1.4±0.5	0.875	32±5	0.993
40	58±2	0.983	150±17	1.8±0.4	0.922	38±2	0.993
60	58±4	0.963	133±8	2.1±0.3	0.934	41±3	0.995
80	69±6	0.986	139±12	2.0±0.4	0.947	47±3	0.996
100	79±6	0.990	145±25	1.9±0.7	0.837	51±2	0.995

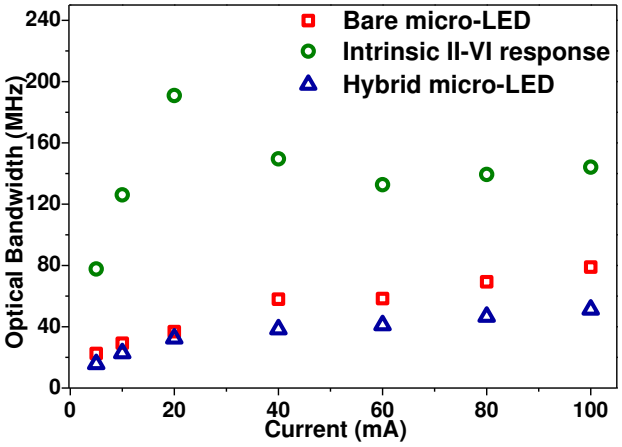

Figure 5. The -3dB optical bandwidths of the bare µLED and of the hybrid micro-LEDs – the intrinsic bandwidth values of the membrane (integrated MQW membrane) are also plotted.

The micro-LED bandwidth is current dependent and reaches 79 MHz at 100 mA. This current dependency can be attributed to the reduced carrier lifetime in the InGaN micro-LED active region as the current, and hence the carrier density, increases [13], [14]. The typical intrinsic response of the membrane is 145 MHz, much faster than conventional phosphors, see also Figure 6. The hybrid micro-LED behavior is the combination of the frequency responses of the color-converting membrane and the underlying micro-LED. The result is a modulation bandwidth of 51 MHz limited by the slower of the two components, i.e. the micro-LED response in this case. Higher modulation bandwidths are expected by using blue micro-LEDs of even smaller dimensions [2].

4.2 Power density dependence of the intrinsic bandwidth of the color-converting membrane

The dependence of the color-converter bandwidth on the incident micro-LED pump power density was further studied. Since the micro-LED is in flip-chip configuration, i.e. the emission occurs through the sapphire substrate, the excitation area at the membrane/sapphire interface is determined by the divergence of the micro-LED light and the propagation length through the sapphire. Due to the small LED size, the excitation spot incident on the membrane can in good approximation be assumed to be circular with diameter equal to the substrate thickness, i.e., 330 +/- 20 µm in this case [15]. The intrinsic bandwidth data of the

membrane as previously determined is then plotted again in Figure 6 as a function of the incident excitation power density ('integrated membrane'). For pump power density between 1 and 1.75 W/cm^2, the average intrinsic bandwidth is 145 MHz.

In order to observe with more confidence the bandwidth behavior of the MQW membrane at excitation power density below 1 W/cm^2, it was independently characterized, i.e. when separated from the micro-LED, as a stand-alone membrane. In this case the membrane was held onto a glass substrate and remotely pumped with a 450nm micro-LED as explained in section 2. Results are plotted in Figure 6 (black squares, 'stand-alone membrane').

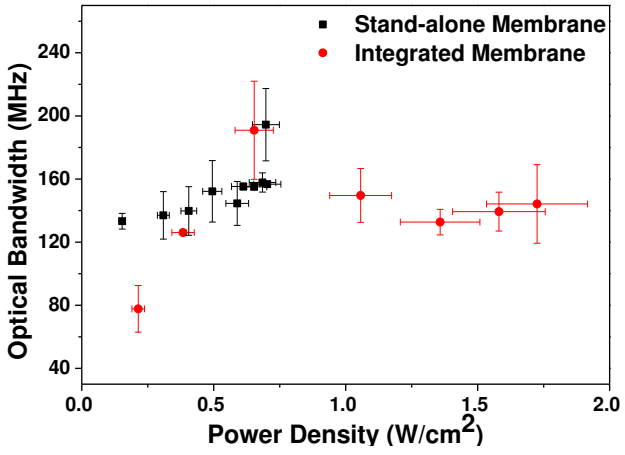

Figure 6. Bandwidth dependence over different power densities.

The vertical error bars in Figure 6 represent the root mean square errors of the fits of the frequency responses. Overall, the presented bandwidth values are within the error bars of the surrounding points so there is no significant power density dependence of the membrane intrinsic bandwidth. The average bandwidth over the range of 450nm light power density corresponding to the operation of the integrated MQW membrane is around 145 MHz. This corresponds to an effective carrier lifetime of 1.9 ns. This value can be corroborated by direct time-correlated single photon counting, TCSPC, measurement of the stand-alone membrane. Such TCSPC analysis was done using an Edinburgh Instruments system using an EPL-450 Picosecond pulsed diode laser as the excitation source (450 nm). Differences in the TCSPC lifetime measurement were seen between membranes processed from the same epilayer structure however, the average measured lifetime from a number of such membranes was found to be 1.4 ± 0.2 ns, showing reasonable consistency with the frequency response data.

The photoluminescence and the optical bandwidth of the MQW membrane, which is two-orders of magnitude higher than for phosphors, means that high-speed color-conversion can be realized for a range of light levels that correspond to micro-LED operation.

5. Conclusions

This proof-of-concept demonstration of a hybrid micro-LED with integrated MQW membrane offers a pathway to fast-response and robust color conversion and has potential for VLC applications. The modulation bandwidth of the 540nm hybrid micro-LED was measured to be up to 51 MHz for an intrinsic bandwidth of the MQW membrane and of the underlying micro-LED of 145MHz and 79 MHz, respectively. Higher modulation bandwidths of the hybrid device are expected by reducing the dimensions of the LED. The integration approach of the membrane by liquid-capillary bonding is well-suited to transfer-printing approaches [16]. It could be extended to other wavelengths using for example MQW structures based on III-V AlGaInP and/or InGaN material systems.

ACKNOWLEDGMENTS

This research work was supported by the EPSRC Programme Grant "Ultra-parallel visible light communications (UP-VLC)" (EP/K00042X/1). The authors would like to acknowledge Dr. Enyuan Xie for the micro-LED fabrication.

REFERENCES

[1] A. Jovicic, J. Li, and T. Richardson, "Visible Light Communication : Opportunities , Challenges and the Path to Market," IEEE Commun. Mag., no. December, pp. 26–32, 2013.

[2] J. J. D. Mckendry, D. Massoubre, S. Zhang, B. R. Rae, R. P. Green, E. Gu, R. K. Henderson, A. E. Kelly, and M. D. Dawson, "Visible-Light Communications

Using a CMOS-Controlled Micro-Light-Emitting-Diode Array," J. Light. Technol., vol. 30, no. 1, pp. 61–67, 2012.
[3] N. Laurand, B. Guilhabert, J. McKendry, A. E. Kelly, B. Rae, D. Massoubre, Z. Gong, E. Gu, R. Henderson, and M. D. Dawson, "Colloidal quantum dot nanocomposites for visible wavelength conversion of modulated optical signals," Opt. Mater. Express, vol. 2, no. 3, p. 250, Feb. 2012.
[4] M. A. Haase, J. Xie, T. A. Ballen, J. Zhang, B. Hao, Z. H. Yang, T. J. Miller, X. Sun, T. L. Smith, and C. A. Leatherdale, "II–VI semiconductor color converters for efficient green, yellow, and red light emitting diodes," Appl. Phys. Lett., vol. 96, no. 23, p. 231116, 2010.
[5] D. Schiavon, M. Binder, A. Loeffler, and M. Peter, "Optically pumped GaInN / GaN multiple quantum wells for the realization of efficient green light-emitting devices," Appl. Phys. Lett., vol. 113509, 2013.
[6] B. Damilano, H. Kim-Chauveau, E. Frayssinet, J. Brault, S. Hussain, K. Lekhal, P. Vennegues, P. De Mierry, and J. Massies, "Metal Organic Vapor Phase Epitaxy of Monolithic Two-Color Light-Emitting Diodes Using an InGaN-Based Light Converter," Appl. Phys. Express, vol. 092105, 2013.
[7] J. J. D. McKendry, R. P. Green, A. E. Kelly, Z. Gong, B. Guilhabert, D. Massoubre, E. Gu, and M. D. Dawson, "High-Speed Visible Light Communications Using Individual Pixels in a Micro Light-Emitting Diode Array," IEEE Photonics Technol. Lett., vol. 22, no. 18, pp. 1346–1348, Sep. 2010.
[8] Z. Gong, S. Jin, Y. Chen, J. McKendry, D. Massoubre, I. M. Watson, E. Gu, and M. D. Dawson, "Size-dependent light output, spectral shift, and self-heating of 400 nm InGaN light-emitting diodes," J. Appl. Phys., vol. 107, no. 1, p. 013103, 2010.
[9] X. Zhou, M. Munoz, M. C. Tamargo, and Y. C. Chen, "Optically pumped laser characteristics of blue Znx′Cdy′Mg1−x′−y′Se/ZnxCdyMg1−x−ySe single quantum well lasers grown on InP," J. Appl. Phys., vol. 95, no. 1, p. 7, 2004.
[10] R. Moug, A. Alfaro-Martinez, L. Peng, T. Garcia, V. Deligiannakis, A. Shen, and M. Tamargo, "Selective etching of InGaAs/InP substrates from II-VI multilayer heterostructures," Phys. Status Solidi, vol. 9, no. 8–9, pp. 1728–1731, Aug. 2012.
[11] Z. L. Liau, "Semiconductor wafer bonding via liquid capillarity," Appl. Phys. Lett., vol. 77, no. 5, p. 651, 2000.
[12] J. R. Lakowicz, G. Laczko, and H. Cherek, "Analysis of Fluorescence decay kinetics form variable-frequency phase shift and modulation data," J. Biophys. Soc., vol. 46, no. October, pp. 463–477, 1984.
[13] E. F. Schubert, Light-Emitting Diodes, 2nd ed. Cambridge University Press, 2006, p. 434.
[14] R. P. Green, J. J. D. McKendry, D. Massoubre, E. Gu, M. D. Dawson, and A. E. Kelly, "Modulation bandwidth studies of recombination processes in blue and green InGaN quantum well micro-light-emitting diodes," Appl. Phys. Lett., vol. 102, no. 9, p. 091103, 2013.
[15] J. Herrnsdorf, Y. Wang, J. J. D. McKendry, Z. Gong, D. Massoubre, B. Guilhabert, G. Tsiminis, G. A. Turnbull, I. D. W. Samuel, N. Laurand, E. Gu, and M. D. Dawson, "Micro-LED pumped polymer laser: A discussion of future pump sources for organic lasers," Laser Photon. Rev., vol. 7, no. 6, pp. 1065–1078, Nov. 2013.
[16] A. J. Trindade, B. Guilhabert, D. Massoubre, D. Zhu, N. Laurand, E. Gu, I. M. Watson, C. J. Humphreys, and M. D. Dawson, "Nanoscale-accuracy transfer printing of ultra-thin AlInGaN light-emitting diodes onto mechanically flexible substrates," Appl. Phys. Lett., vol. 103, no. 25, p. 253302, 2013.